

## A Thymine Isostere in the Templating Position Disrupts Assembly of the Closed DNA Polymerase $\beta$ Ternary Complex

Thomas W. Kirby, Eugene F. DeRose, William A. Beard, Samuel H. Wilson, and Robert E. London\*

Laboratory of Structural Biology, National Institute of Environmental Health Sciences, National Institutes of Health, Research Triangle Park, North Carolina 27709

Received June 17, 2005; Revised Manuscript Received September 12, 2005

**ABSTRACT:** The high fidelity of the DNA polymerization process is critically important for the stability of the cellular genome. The role of template and incoming nucleotide base pairing in polymerase fidelity has recently been explored by the use of nucleotide isosteres, which preserve the steric but not the electronic properties of the corresponding bases. The DNA repair enzyme, DNA polymerase  $\beta$  (Pol  $\beta$ ), is among the most discriminating, being inactive when the thymine isostere difluorotoluene (DFT) is present in the templating base position. To explore the physical basis for this inactivity, we have performed NMR studies on [*methyl*- $^{13}\text{C}$ ]methionine-labeled Pol  $\beta$  complexed with double-hairpin DNA, used to model the gapped nucleotide substrate, and having either a thymine or a DFT isostere at the templating base position. The six methionine residues distributed throughout the enzyme provide useful conformational probes of the lyase and polymerase domains and subdomains. Analysis of the proton shift of Met282 that results from formation of an abortive Pol  $\beta$ –gapped DNA–dATP complex is consistent with an open to closed conformational change of the enzyme predicted from crystal structures. In contrast, the same resonance is nearly unshifted when a ternary complex is formed from dATP and gapped DNA in which a DFT isostere replaces thymine at the templating base position. Alternatively, the resonances of Met191 and Met155, located in the catalytic subdomain, show perturbations upon formation of the abortive ternary complex, which are qualitatively similar, but significantly weaker, than the changes observed when thymine is present at the templating base position. The changes in the Met155 and Met191 methyl resonances are in fact more similar to those observed in the binary Pol  $\beta$ –dATP complex. These studies demonstrate that the block in catalysis is directly related to the absence of the set of conformational transitions that include the “open” to “closed” transition monitored by Met282.

An understanding of the structural, thermodynamic, and kinetic factors that govern the fidelity of DNA polymerization is central to our understanding of mutagenesis and mutation-related diseases. DNA polymerase  $\beta$  (Pol  $\beta$ ),<sup>1</sup> a member of the X-family of DNA polymerases, contributes two enzymatic activities to the repair of simple base lesions during mammalian base excision repair. These activities, DNA synthesis and 5'-deoxyribose phosphate removal (dRP lyase), are found on distinct domains. The 8 kDa amino-terminal lyase domain is tethered to the 31 kDa polymerase domain by a short hinge region (1). The polymerase domain is further composed of functionally distinct subdomains. These domains and subdomains undergo large conformational changes upon substrate binding. In addition, numerous subtle substrate and protein side chain adjustments occur (2–5). Pol  $\beta$  has proven to be a particularly useful system for studying the conformational and catalytic events related to DNA synthesis (6–8). In addition to the series of crystallographic studies that demonstrate the structural changes that accompany the

polymerization process (2), we have recently shown that NMR studies of selectively labeled Pol  $\beta$  provide a useful approach for the analysis of the conformational properties of the enzyme in solution (8).

DNA polymerase  $\beta$  binds the 5'-phosphate in gapped DNA through the positively charged side chains in its lyase domain (9). If the 3'-OH of the primer strand is nearby (i.e.,  $\leq 5$  nucleotides), the polymerase domain can engage the primer terminus. In the crystal structure of the binary complex of Pol  $\beta$  with single-nucleotide gapped DNA, the carboxyl-terminal N-subdomain<sup>2</sup> of Pol  $\beta$  is positioned in a conformation that opens the nascent base pair binding pocket. Addition of the correct nucleoside triphosphate (dNTP) allows the enzyme to reposition the N-subdomain, forming a closed binding pocket around the incoming dNTP and the templating base. Formation of the closed ternary complex coincides with an increase in the binding affinity for both DNA and dNTP (7). We have correlated these structural and catalytic events with conformational changes monitored by methionine residues distributed in the lyase domain and N- and C-subdomains of Pol  $\beta$  (Met18 in the lyase domain, Met155,

\* To whom correspondence should be addressed: MR-01, Laboratory of Structural Biology, NIEHS, 111 Alexander Dr., Research Triangle Park, NC 27709. Phone: (919) 541-4879. Fax: (919) 541-5707. E-mail: london@niehs.nih.gov.

<sup>1</sup> Abbreviations: DFT, 2,4-difluorotoluene; DSS, 2,2-dimethylsilapentane-5-sulfonic acid; Pol  $\beta$ , DNA polymerase  $\beta$ ; dNTP, 2'-deoxynucleoside 5'-triphosphate.

<sup>2</sup> We employ a functionally based nomenclature for the polymerase domain (35). The N- and C-subdomains correspond to the fingers and palm subdomains, respectively, where an architectural analogy to a right hand is used.

Met158, Met191, and Met236 in the C-subdomain, and Met282 in the N-subdomain) (8).

Watson–Crick hydrogen bonding plays a crucial role in stabilizing the structure of DNA. However, the role of these hydrogen bonds for substrate discrimination during DNA synthesis is unclear. Kool and co-workers have demonstrated the utility of fluorinated nucleoside isosteres for separating the contributions of hydrogen bonding at the Watson–Crick edge and minor groove of the nascent base pair from steric and geometric constraints imposed by the nascent base pair binding pocket (10). Studies utilizing the thymine isostere 2,4-difluorotoluene (DFT) have demonstrated that the contribution of hydrogen bonding interactions between the bases of the nascent base pair and the polymerase varies significantly depending on the polymerase under investigation. For Pol  $\beta$ , the presence of the DFT isostere in the templating position fails to support polymerization (11). To interpret the observed kinetic differences, it is important to understand the molecular basis for this effect, and the reason for the significant variation observed among different polymerases in their ability to use this base analogue as a substrate.

In this study, we have utilized [*methyl*- $^{13}\text{C}$ ]methionine-labeled Pol  $\beta$  to probe the conformational response of the enzyme to homologous substrates containing either thymine or DFT at the templating base position. As shown previously (8), the six methionine residues of Pol  $\beta$  (excluding the amino-terminal methionine) provide useful and specific information about the response of different regions of the enzyme to substrate binding, leading to structural and dynamic insights into their potential kinetic and thermodynamic consequences. While in the previous studies we achieved the formation of an abortive ternary complex by the serial addition of templating DNA, downstream oligonucleotide, primer DNA, and chain-terminating dideoxy nucleoside triphosphate, in this study we have made use of a double-hairpin substrate that eliminates the need for stepwise addition of the DNA and ensures accurate stoichiometry. The ability to correlate dynamic conformational changes with kinetic and thermodynamic consequences remains a challenge with all enzyme systems, but the results described here provide insight into the microscopic events that precede catalysis.

## EXPERIMENTAL PROCEDURES

**Materials.** The [*methyl*- $^{13}\text{C}$ ]methionine-labeled rat Pol  $\beta$  was prepared as described previously (8) by growth of the plasmid-containing *Escherichia coli* on a medium containing [*methyl*- $^{13}\text{C}$ ]methionine (CIL, Cambridge, MA). NMR samples contained 0.3–0.6 mM Pol  $\beta$  in a  $\text{D}_2\text{O}$  buffer consisting of 40 mM Tris- $d_{11}$  (pH 7.6), 130 mM KCl, 1 mM DTT, 0.1 mM AEBSEF, 0.04%  $\text{NaN}_3$ , and 50  $\mu\text{M}$  DSS as an internal chemical shift standard. Oligonucleotides, including one containing a difluorotoluene isostere (The Midland Certified Reagent Co., Midland, TX), were dissolved in  $\text{D}_2\text{O}$  to make  $\sim 15$  mM stock solutions. The difluorotoluene-containing nucleoside isostere is the C-nucleoside, 5-[1'-(2'-deoxy- $\beta$ -D-ribofuranosyl)]-2,4-difluorotoluene, the synthesis of which has been described by Schweitzer and Kool (12).

The protein concentration was determined using an extinction coefficient of  $20\,088\text{ M}^{-1}\text{ cm}^{-1}$  at 280 nm, and the DNA concentrations for the T-hairpin and DFT-hairpin were

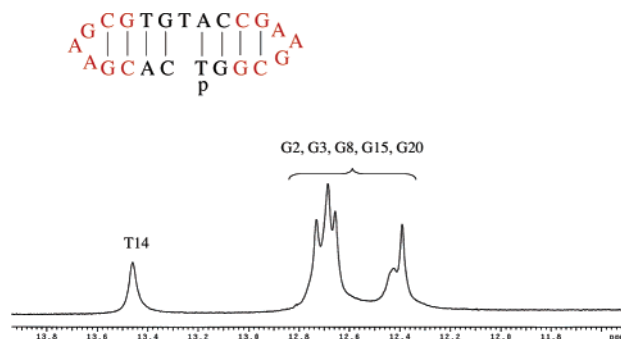


FIGURE 1: Imino region of the  $^1\text{H}$  NMR spectrum of the double-hairpin DNA substrate (inset) used to generate the [*methyl*- $^{13}\text{C}$ ]methionine Pol  $\beta$ –DNA complex shown in Figure 2. The spectrum was obtained at 25  $^\circ\text{C}$  in the NMR buffer given in Experimental Procedures. The seven-residue Hirao turn is colored red.

determined using extinction coefficients of  $211\,600$  and  $245\,100\text{ M}^{-1}\text{ cm}^{-1}$  at 260 nm, respectively.

**NMR Spectroscopy.** NMR experiments were performed at 25  $^\circ\text{C}$  on a Varian UNITY INOVA 600 MHz NMR spectrometer, using a 5 mm Varian (600 MHz)  $^1\text{H}\{^{13}\text{C},^{15}\text{N}\}$  triple-resonance probe, equipped with actively shielded Z-gradients. The  $^1\text{H}$ – $^{13}\text{C}$  HSQC spectra were acquired using Varian's gChsqc sequence (13). The data were acquired as a  $230 (t_1) \times 512 (t_2)$  complex matrix, with acquisition times of 63.9 ( $t_1$ ) and 64.0 ms ( $t_2$ ), 128 scans per increment, and a 1.0 s delay between scans. The spectra were processed using NMRPipe version 2.1 (14) and analyzed using NMRView version 5.0.4 (15). All spectra were processed using squared cosine bell apodization functions in all dimensions and forward–backward linear prediction in the indirect  $^{13}\text{C}$  dimension (16).

**Chemical Shift Predictions.** Theoretical shift calculations for the methyl proton resonances of the labeled methionine residues were performed using either ShiftX version 1.1 (17), available at <http://redpoll.pharmacy.ualberta.ca/shiftx/>, or SHIFTS version 4.1 (18, 19), available at <http://www.scripps.edu/mb/case/qshifts/qshifts.htm>. The input data consisted of the protein coordinates for Protein Data Bank (PDB) entries 1BPX and 1BPY (2) or the coordinates of a recently obtained 1.65  $\text{\AA}$  resolution structure of a Pol  $\beta$  ternary complex (J. M. Krahn and S. H. Wilson, unpublished results). DNA coordinates were not included in the input, since in a few cases the program did not execute when these were present. The DNA is anticipated to contribute primarily to the shift of Met236, which makes contact with the primer terminus. The programs do not predict  $^{13}\text{C}$  shift values for the side chains.

## RESULTS

**Response of Pol  $\beta$  to Double-Hairpin DNA.** In our previous study (8), we achieved the formation of an abortive ternary complex by the serial addition of templating DNA, primer and downstream oligonucleotides that create a gap, and chain-terminating dideoxynucleoside triphosphate. Here, we have made use of a double-hairpin DNA substrate that eliminates the need for stepwise addition of three oligonucleotides, ensuring accurate stoichiometry. The double-hairpin DNA substrates used in this study were based on the high stability of the compact seven-nucleotide hairpin first described by Hirao et al. (20) (Figure 1). In this DNA,

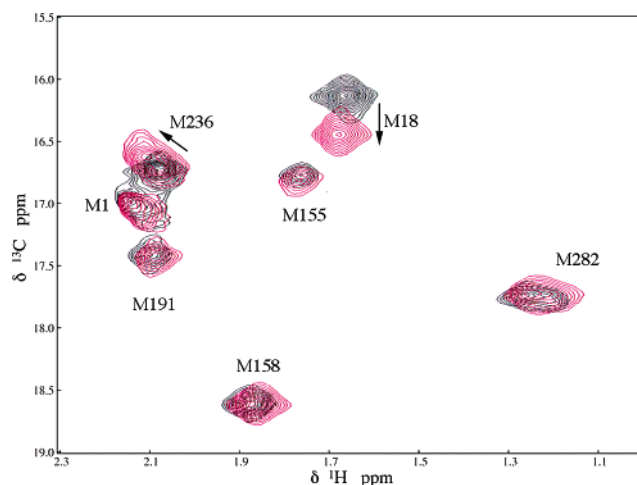


FIGURE 2: Spectrum of [*methyl*- $^{13}\text{C}$ ]methionine-labeled Pol  $\beta$  characterized by seven methyl resonances (including Met1, M1). Addition of the double hairpin shown in Figure 1 produces shifts for Met18 (M18) due to the interaction with the downstream portion of the DNA, and Met236 (M236), which interacts with the primer terminus. The  $^1\text{H}$ – $^{13}\text{C}$  HSQC spectrum of the apoenzyme is colored black, and the spectrum of the complex with the double-hairpin is colored magenta.

the sequence spanning the central nucleotide gap is flanked on either side by a 5'-GCGAAGC heptamer that forms a high-stability turn. The double-hairpin structure has previously been used to investigate the interactions of nicked DNA substrates (21). The imino region of the  $^1\text{H}$  NMR spectrum obtained for the oligonucleotide 5'-p-TGGCGAAGCCAT-GTGCGAAGCAC-3' reveals the expected low-field imino proton resonances, with the exception of the terminal base pairs which are subject to fraying effects (Figure 1). The high stability of the double-hairpin DNA structure obtained using the Hirao heptamer, and the relatively short length of the central structure, greatly reduce the problem of intermolecular extensions that could occur with self-complementary DNA.

We previously assigned the methionine methyl resonances of Pol  $\beta$  and analyzed the effects of the serial addition of a template, 5'-phosphorylated downstream, and primer oligonucleotides and a correct incoming nucleotide on enzyme conformation, as monitored by these resonances (8). The  $^1\text{H}$ – $^{13}\text{C}$  HSQC spectra obtained for the complex formed from the hairpin illustrated in Figure 1 with [*methyl*- $^{13}\text{C}$ ]methionine Pol  $\beta$  are consistent with our previous study (Figure 2). Specifically, binding of the gapped DNA double-hairpin DNA substrate leads to a significant shift of the Met18 resonance ( $\Delta^{13}\text{C} = 0.35$  ppm), and to smaller shifts of Met236, which comes in contact with the nucleotide at the primer terminus (8). The remaining methionine methyl resonances exhibit small or negligible shifts. These results demonstrate that, from the standpoint of the methionine residues in Pol  $\beta$ , the addition of the double-hairpin DNA results in essentially the same conformational alterations that are produced by the serial addition of the template, primer, and downstream oligonucleotides.

To create ternary complexes, we employed double-hairpin DNA substrates containing a two-nucleotide gap with G and T residues at the unpaired templating positions (Figure 3). As a result of template-directed ddCTP insertion, Pol  $\beta$  creates a single-nucleotide gap with a dideoxycytidine residue

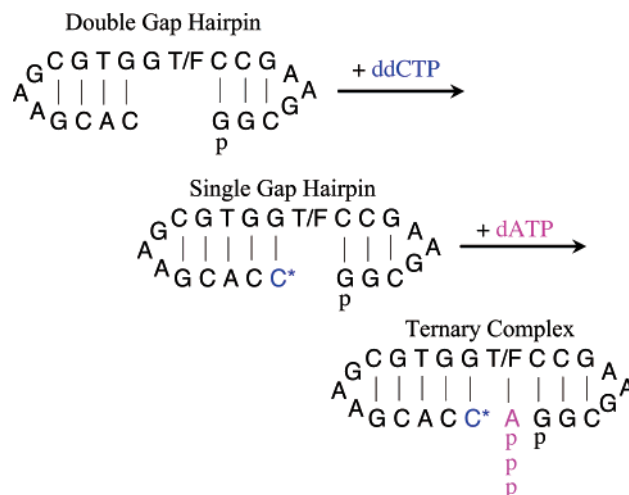


FIGURE 3: DNA double-hairpin sequences used in these studies form a two-nucleotide gap with a 5'-phosphate group. The T/F designation in the gap corresponds to either thymine (T-hairpin) or the difluorotoluene isostere (DFT-hairpin). The structure is converted to a dideoxy-terminated, single-nucleotide gap by Pol  $\beta$  after the addition of ddCTP (blue). The subsequent addition of dATP (magenta) creates an abortive ternary complex.

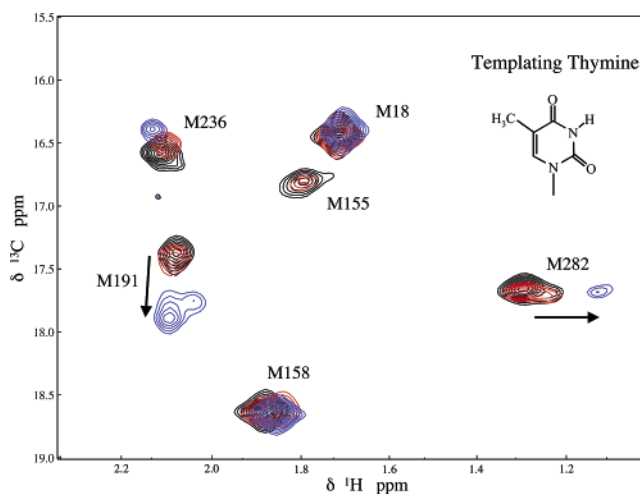


FIGURE 4:  $^1\text{H}$ – $^{13}\text{C}$  HSQC spectra of [*methyl*- $^{13}\text{C}$ ]methionine Pol  $\beta$  in the presence of the double-hairpin DNA substrate (T-hairpin, thymine in the gap). The spectrum of the 1:1 binary complex of Pol  $\beta$  with the double-hairpin DNA containing a two-nucleotide gap is colored black; the spectrum of the binary polymerase–DNA complex formed after addition of ddCTP to generate a single-nucleotide gap is colored red, and the spectrum of the abortive ternary complex formed after the subsequent addition of dATP is colored blue. The structure of the templating thymine base is shown (inset).

at the primer 3'-terminus. The subsequent addition of dATP results in an abortive ternary complex. The resulting  $^1\text{H}$ – $^{13}\text{C}$  HSQC spectra corresponding to the Pol  $\beta$  complex with the original double hairpin, the primer-terminated hairpin, and the abortive ternary complex are shown in Figure 4. As can be seen in Figure 4, the methyl resonance for Met18, which is sensitive to formation of the initial DNA complex, is insensitive to the differences among the DNA molecules shown in Figure 3, and the peak for Met158 is essentially unchanged as well. These results are identical with those of the previous studies using three oligonucleotides to produce the gapped DNA substrate. Additionally, each complex is characterized by small shifts in the resonance of Met236, consistent with the position of this residue near the primer



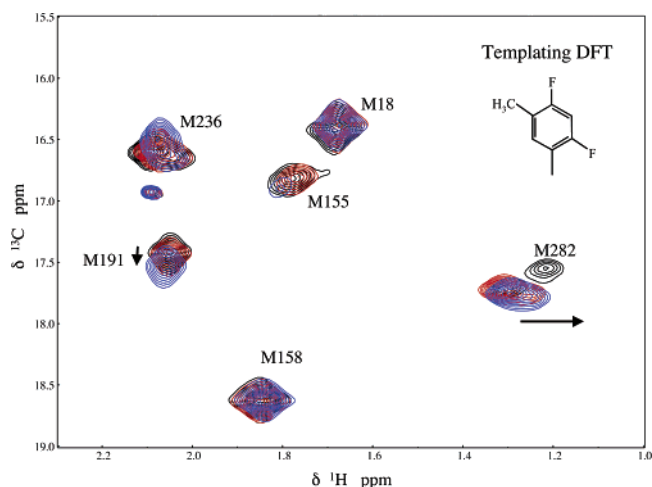


FIGURE 5:  $^1\text{H}$ – $^{13}\text{C}$  HSQC spectra of [methyl- $^{13}\text{C}$ ]methionine Pol  $\beta$  in the presence of the double-hairpin DNA substrate (DFT-hairpin, DFT in the gap). The spectrum of the 1:1 binary complex of Pol  $\beta$  with double-hairpin DNA containing a two-nucleotide gap is colored black; the spectrum of the binary complex after addition of ddCTP to generate a single-nucleotide gap is colored red, and the spectrum of the abortive ternary complex formed after addition of dATP is colored blue. The structure of the templating DFT base is shown (inset).

3'-terminus. It is interesting to note that the shifts for this residue, which makes direct contact with the DNA, are generally smaller than those of Met191 and Met282 that result from indirect, conformational changes in the enzyme. Formation of the abortive ternary complex results in the same spectral perturbations noted earlier (8): significant broadening of Met155, a downfield shift of Met191 primarily in the  $^{13}\text{C}$  dimension ( $\Delta^{13}\text{C} = 0.49$  ppm), and an upfield shift and broadening of the Met282 resonance, primarily in the  $^1\text{H}$  dimension ( $\Delta^1\text{H} = 0.18$  ppm). We note here that, as in our previous study (8), the Met282 resonance exhibits an upfield shoulder in the  $^1\text{H}$  dimension, the significance of which is at present unknown. There is also a small shift for Met236, as noted above. In summary, all of the methionine resonance perturbations observed in the presence of the double hairpin are identical with those achieved by the serial addition of template, primer, and downstream oligonucleotides to create an equivalent gapped DNA substrate.

**Effect of the Difluorotoluene Isostere.** The series of studies described above was repeated with a double-hairpin DNA substrate in which the templating thymidine nucleoside used in the first series was replaced with a difluorotoluene-containing nucleoside. Unexpectedly, the complex formed with the double hairpin containing a two-nucleotide gap exhibited a perturbed shift for Met282 (Figure 5). This shift may indicate a significant variation of the interaction of the DFT with the adjacent Arg283 residue (see Discussion). Formation of the single-nucleotide gap substrate after addition of the ddCTP resulted in a spectrum more similar to that observed previously (cf. Figures 4 and 5) (8). In dramatic contrast with the results obtained for the double-hairpin substrate with thymine at the templating base position, addition of dATP did not produce a significant shift for the Met282 resonance. As discussed previously (8), Met282 provides an important probe of the conformation of the N-subdomain that undergoes a large conformational transition in going from the open binary complex to the closed ternary complex. In contrast with the absence of a Met282 shift,

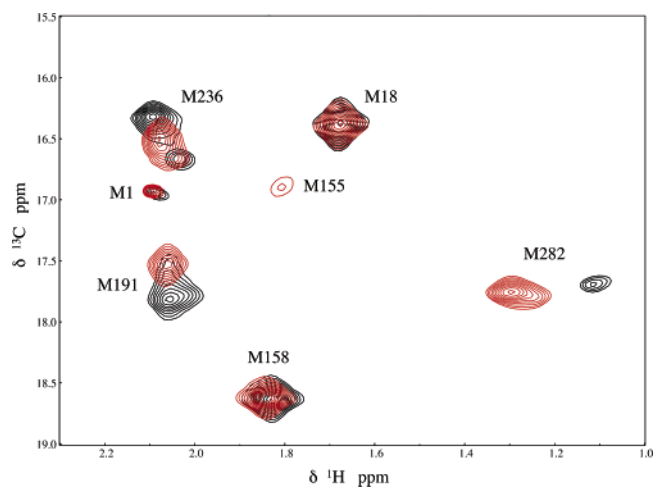


FIGURE 6:  $^1\text{H}$ – $^{13}\text{C}$  HSQC spectra of [methyl- $^{13}\text{C}$ ]methionine Pol  $\beta$  comparing the effects of the abortive ternary complexes formed from the two hairpin DNA substrates: T-hairpin (black) and DFT-hairpin (red). The further addition of the DNA ligand significantly reduced the size of the unshifted resonance (see the Supporting Information).

smaller shifts for Met191 and some broadening of the Met155 resonance are observed for this ternary complex. As shown previously, the addition of dATP in the absence of DNA tends to produce similar shifts, presumably resulting from formation of a weak complex with Pol  $\beta$  (8). Thus, the pattern observed resembles that produced by the addition of a dNTP in the absence of the DNA substrate. The results therefore demonstrate that the poor catalytic activity of Pol  $\beta$  obtained when the DFT isostere is situated at the templating base position is correlated with the absence of the significant conformational change which accompanies formation of the closed ternary complex.

The different effects of the two substrates on enzyme conformation as monitored by the methionine resonances are most clearly illustrated by a superposition of the spectra corresponding to the two ternary complexes (Figure 6). The Met155 resonance is significantly broadened even in the complex formed with the DFT-containing substrate, but with the thymine-containing substrate, it is broadened more such that it is below the threshold used to illustrate complex formation. The different extent of the Met191 shifts is also clearly apparent from the figure. The methyl resonance of Met282 is significantly shifted and broadened in the ternary complex formed from the T-hairpin, but minimally affected by formation of the ternary complex from the DFT-hairpin. As is apparent from Figure 6, in the T-hairpin ternary complex, Met236 corresponds to two component resonances; the observation of two resonances arising from this residue could indicate conformational heterogeneity or incomplete saturation, or it could arise from heterogeneity in either the DNA or enzyme preparation. We were able to eliminate nearly all of the unshifted Met236 resonance by increasing the concentration of the DNA significantly beyond stoichiometric equality, suggesting that DNA heterogeneity may be the basis for this observation (Supporting Information).

**Structural Interpretation of Methionine Resonance Shifts.** As observed in these studies with the double-hairpin DNA (i.e., T-hairpin), and in our previous report (8) using three oligonucleotides to generate a gapped DNA substrate, formation of an abortive ternary complex results in an upfield

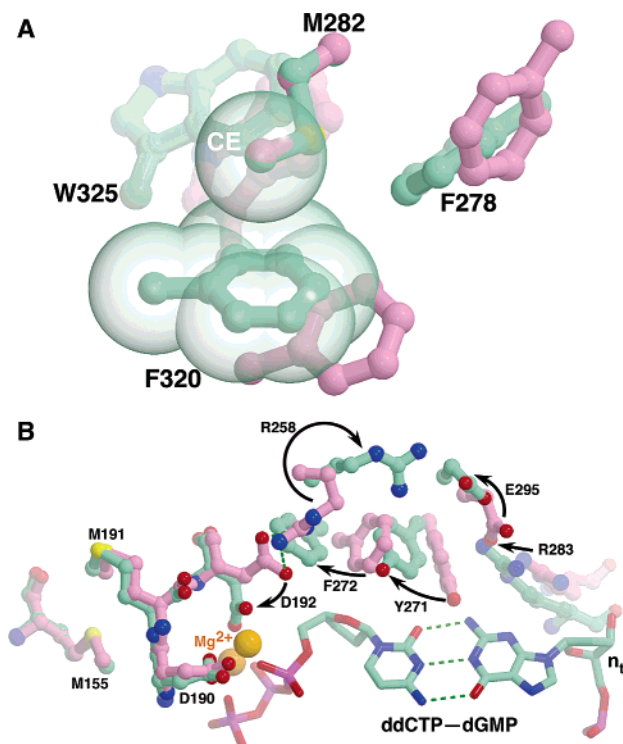


FIGURE 7: Structural changes of Pol  $\beta$  related to ternary complex formation. (A) The region around the C $\epsilon$  of Met282 (CE) in the crystallographic open complex (binary, mauve) is compared to that observed in the closed (ternary) complex of Pol  $\beta$  (green, 2). The Met282 side chains were aligned to make this comparison. The altered conformations of several neighboring aromatic residues (Phe278, Trp325, and particularly Phe320) are consistent with the observed shifts. (B) Transmission of information from the nascent base pair to the catalytic subdomain. In the closed abortive ternary complex (green), Met155 is situated near the active site DMD motif, the active site Mg<sup>2+</sup> ions (orange) that are coordinated by conserved carboxylates (only Asp190 and Asp192 shown), and the triphosphate of the incoming nucleotide (ddCTP). In this conformation, Arg283 makes van der Waals contact with the minor groove edge of the templating base ( $n_i$ ) and forms a hydrogen bond with the sugar of the  $n - 1$  templating nucleotide (not shown). In the binary DNA complex (mauve),  $\alpha$ -helix N (residues 276–288) is displaced from the DNA substrate precluding direct interactions. Formation of the ternary complex results in the series of conformational changes that is illustrated.

proton shift of  $\sim 0.2$  ppm for the Met282 methyl resonance. A comparison of the reported crystal structures of the Pol  $\beta$ -gapped DNA binary complex (PDB entry 1BPX) with that of an abortive ternary complex (PDB entry 1BPY) (2) reveals a number of major conformational changes, including a rotation of  $\alpha$ -helix N (residues 276–288) about an axis through  $\alpha$ -helix M. This closing motion, associated with binding of a correct nucleotide, results in critical interactions between Arg283 and the templating base, thereby significantly altering the local environment of Met282. A comparison of the environment of the Met282 side chain between the open binary structure, corresponding to the complex with single-nucleotide gapped DNA, and the closed abortive ternary complex structure is shown in Figure 7A. From a chemical shift standpoint, the most significant change appears to be a relative movement that places the Met282 methyl group directly above the Phe320 aromatic ring. The mean height of the Met282 methyl protons above the Phe320 ring decreases by 0.74 Å, and the mean distance from the center of the ring decreases from 3.3 to 0.9 Å in going from the

Table 1: Theoretical <sup>1</sup>H Shift Values and Differences for the Indicated Crystal Structures

residue	calculated shift value				
	1BPX	1BPY	pol $\beta$ – TC <sup>a</sup>	1BPY – 1BPX	pol $\beta$ TC – 1BPX
Calculations Using ShiftX, Version 1.1 (17)					
Met18	2.15	2.42	2.09	0.27	–0.06
Met155	2.22	2.23	2.26	0.01	0.04
Met158	2.03	2.05	2.13	0.02	0.10
Met191	1.79	1.82	1.76	0.03	–0.03
Met236	2.02	2.13	2.11	0.11	0.09
Met282	1.95	1.55	1.36	–0.40	–0.59
rmsd <sup>b</sup>				0.20	0.24
Calculations Using SHIFTS, Version 4.1 (18, 19)					
Met18	1.99	2.06	1.81	0.07	–0.18
Met155	1.74	1.76	2.01	0.02	0.27
Met158	1.79	1.41	1.90	–0.38	0.11
Met191	1.74	1.81	1.73	0.07	–0.01
Met236	1.93	2.10	1.89	0.17	–0.04
Met282	1.70	1.32	1.18	–0.38	–0.52
rmsd <sup>b</sup>				0.22	0.25

<sup>a</sup> Unpublished 1.65 Å resolution structure of a Pol  $\beta$  ternary complex (J. M. Krahn and S. H. Wilson, unpublished study). <sup>b</sup> The rmsd values were calculated from the relationship  $\text{rmsd} = \sqrt{\sum_{i=1,6}^{1/6} (\Delta_i - \Delta_{\text{mean}})^2}$ , where the summation is over the results for the six methionine residues.

open binary to the closed ternary complex. This suggests that, at least qualitatively, formation of the ternary complex would be accompanied by an upfield shift of the Met282 methyl resonance, as is observed.

The above interpretation is further supported by theoretical shift calculations using ShiftX by Neal et al., which computes shifts from structural data (17). Methyl proton shifts for the methionine resonances of a binary complex of Pol  $\beta$  with gapped DNA (computed from the coordinates of PDB entry 1BPX), an abortive ternary complex (computed from the coordinates of PDB entry 1BPY), and a second high-resolution ternary complex (1.65 Å) (J. M. Krahn and S. H. Wilson, unpublished results) are summarized in Table 1. In general, the small range of the methionine methyl proton shifts limits the utility of this approach; however, a significant upfield shift for the Met282 methyl protons is predicted for both ternary complexes. This predicted shift is greater than twice the rmsd value for all of the methionine shifts. Qualitatively similar results were obtained using SHIFTS by Xu and Case (18, 19), and for this calculation, the shift contribution can be attributed to the ring current term in the calculation. We note that all of the calculations in Table 1 give qualitatively consistent upfield shift predictions for the Met282 methyl proton resonance, and the predicted shifts for Met158 and Met18 seen in Table 1 are not consistent among the calculations, indicating that a substantial reason for this variation is the variability of the crystal structure coordinates used, and secondarily, a variation in the theoretical approaches followed. As discussed previously (8), the B-factors for the methionine methyl groups in these structures are generally large, particularly for Met18 and Met155.

In addition to the predictions for Met282, both programs predict a very small (+0.02 ppm) shift for the proton methyl resonance of Met155, while the experimental results show that formation of the ternary complex is accompanied by significant broadening of the corresponding methyl resonance. These results indicate that either (1) concomitant with

the closing subdomain motion is a very large  $^{13}\text{C}$  shift which may result in the exchange broadening observed for the Met155 resonance or (2) the ternary complex observed in solution does not correspond closely to the crystal structure, but to a more complex mixture of structures.

## DISCUSSION

DNA polymerase  $\beta$  plays an important role in the repair of short gaps in the DNA polymer and has also served as a useful model for understanding the relationships among structure, dynamics, and DNA synthesis fidelity. To achieve high-fidelity polymerization, information about the structure of the nascent base pair must be transmitted many angstroms to the catalytic, or nucleotidyl transfer site of the enzyme. This is believed to occur through an induced-fit mechanism where the enzyme forms an active conformation with the correct nascent base pair, but forms a less active conformation(s) with an incorrect base pair (2, 22–24). It is generally assumed that the closed ternary complex represents the “active” conformation and is generally defined from the position of  $\alpha$ -helix N of the N-subdomain. However, the position of the N-subdomain does not always define the active conformation since crystallographic structures of unliganded forms of Y-family DNA polymerases (25) and a DNA complex of DNA polymerase  $\lambda$  (26), an X-family DNA polymerase, indicate that the N-subdomain is in a position reminiscent of the closed conformation. However, the liganded structures of these polymerases do not indicate that their nascent base pair binding pockets are closed as suggested by the position of the N-subdomain. More importantly, there are numerous subtle protein and substrate conformational changes that are necessary for formation of an active ternary complex (1–6). These observations highlight the importance of defining local conformational changes during catalytic activation rather than global protein structural transitions alone.

Replacement of a templating thymidine with the DFT-containing nucleoside isostere creates a subtle change in the nucleotide by preserving the steric characteristics of the thymine base while eliminating the capability for forming hydrogen bonds with the incoming nucleoside triphosphate and DNA polymerase. Moran and Kool (27, 28) first described the efficient and specific replication of difluorotoluene by an exonuclease-deficient mutant of the Klenow fragment of *E. coli* DNA polymerase I. This observation suggested that, at least for this A-family DNA polymerase, Watson–Crick and polymerase–template nucleotide hydrogen bonding were apparently dispensable during substrate discrimination. In contrast, Morales and Kool (11) later found that Pol  $\beta$  did not support the insertion of the sterically complementary dATP opposite DFT. We sought to investigate the structural basis for this observation using NMR studies of [*methyl*- $^{13}\text{C}$ ]methionine Pol  $\beta$ . We have previously demonstrated that the methionine residues of Pol  $\beta$  can provide a useful set of probes for conformational changes and dynamic behavior of this enzyme. Thus, the resonance of Met18, located in the amino-terminal lyase domain, is sensitive to the binding of single-stranded DNA and particularly to the addition of a complementary, 5'-phosphorylated oligonucleotide, but is insensitive to the presence of a primer strand or to the formation of a ternary complex (8). This was consistent with previous biochemical studies (2,

9). Alternatively, the methyl resonance of Met282, located at the center of  $\alpha$ -helix N of the N-subdomain, exhibits a significant shift upon formation of an abortive ternary complex. Comparison of the  $^1\text{H}$  shift of the Met282 methyl resonance with theoretical predictions using ShiftX (17) and SHIFTS (18, 19) supports the conclusion that the observed shift corresponds to a conformational change similar to that observed in the crystal structure of the closed ternary Pol  $\beta$ -gapped DNA–dNTP complex (2).

A comparison of the spectral perturbations that result from formation of the abortive ternary complexes with the T-hairpin, which contains a thymine base at the template position, and the DFT-hairpin, which contains a difluorotoluene at the template position, provides some support for an induced fit mechanism. As discussed previously and observed again in this study using a double hairpin, formation of an abortive ternary Pol  $\beta$ -gapped DNA–dNTP complex results in three major spectral perturbations: an upfield  $^1\text{H}$  shift of the Met282 methyl resonance, a downfield  $^{13}\text{C}$  shift of the Met191 methyl resonance, and a significant broadening of the Met155 methyl resonance (Figure 4). Qualitatively similar but substantially smaller effects are observed with the corresponding ternary complex formed with the DFT-hairpin. If we set the total change for each of the above spectral perturbations observed with the T-hairpin to 100%, then the ternary complex with the DFT-hairpin produces 11% of the effect on Met282, and 23% of the effects on Met155 and Met191. This result suggests that the enzyme does not respond as a rigid entity. The larger perturbation of the resonances in the catalytic C-subdomain may reflect a specific interaction with the dNTP ligand. Thus, we noted previously that the binding of a dNTP to Pol  $\beta$  in the absence of DNA produced selective perturbations of the C-subdomain methionine methyl resonances that were qualitatively similar to those observed in the ternary complex, but much smaller in magnitude.

Although the analysis given above sets the NMR parameters determined in the ternary Pol  $\beta$ -T-hairpin–dATP perturbation at 100%, this does not mean that this complex corresponds to a pure state. In particular, the extreme broadening of the methyl resonance of Met155 indicates the presence of significant conformational exchange in the fully complexed polymerase. Since Met155 is near the triphosphate-binding site for the incoming nucleotide (Figure 7B), the perturbation of this resonance in the ternary complex probably indicates that dATP binding occurs when the templating base is DFT. As discussed previously, there is no specific information about the nature of the conformational states related to the observed broadening. They may be related to the open and closed conformations observed in the crystal structures, and/or they may correspond to the attempt of the enzyme to form a catalytically active complex. Some of the larger conformational changes coupling the templating base–Arg283 interaction with residues in the active site are illustrated in Figure 7B. It is interesting to note that, as shown in Figure 7B, the Met155 methyl group is positioned near the backbone of the DMD active site motif. This position suggests that millisecond to microsecond time scale dynamic behavior at the active site of the abortive ternary complex may be the basis for the observed resonance broadening. As noted previously (8), the broadening of the resonance is consistent with the elevated *B*-factor observed



for Met155 in the crystallographic structure of the ternary complex as compared to that of the apoenzyme or the binary DNA complex. Thus, although abortive ternary complex formation can lead to tight substrate binding with localized restricted motions, there are other regions that become more dynamic on the microsecond to millisecond time scale. Molecular modeling of the N-subdomain opening and closing motions of Pol  $\beta$  has suggested that molecular rearrangements must occur after subdomain closure for catalytic activation to occur (5, 29). How these motions influence or facilitate catalytic activation remains an important and challenging question.

Interestingly, the complex formed with the double hairpin containing a two-nucleotide gap exhibited a perturbed shift for Met282 when DFT was in the gap (Figure 5, black). This may reflect an alternate conformation of the adjacent Arg283 when the hydrophobic base analogue replaces thymine. In the open binary single-nucleotide gap DNA complex, Arg283 is solvent-exposed. However, in the closed ternary complex, Arg283 interacts with the templating base and sugar of the upstream (i.e., 3') templating nucleotide. Alanine substitution for Arg283 (R283A) dramatically decreases the catalytic efficiency of correct nucleotide insertion (30, 31), base substitution fidelity (30, 32), and frameshift fidelity (33). Although a binary complex structure for Pol  $\beta$  with a DNA substrate containing a two-nucleotide gap has not been determined, a binary complex structure of DNA polymerase  $\lambda$ , a closely related X-family DNA polymerase, bound to a two-nucleotide gap indicates that the equivalent arginine, Arg517, forms van der Waals interactions with the templating base (26). This observation suggests that the observed shift with DFT may reflect an alternate conformation of Arg283 that is transmitted to Met282.

Pol  $\beta$  senses the formation of the nascent base pair via several interactions, among them, the interaction of the methylene side chain of Arg283 with the templating base and a hydrogen bond between NH-1 of Arg283 and the sugar group of the penultimate template strand nucleotide (Figure 7B). We conclude that the failure of the incoming dATP base to properly interact with DFT is sufficiently serious such that the normal templating base–Arg283 interactions fail. The failure of these interactions is in turn transmitted to the catalytic process by virtue of Arg283's inability to form the contact with the sugar group of the penultimate nucleotide of the template strand (Figure 7B). A prediction stemming from this interpretation is that a crystal structure of a ternary complex with DFT in the templating base position and dATP as the incoming nucleotide will correspond to an open or intermediate conformation for the N-subdomain, rather than the closed conformation observed with a Watson–Crick nascent base pair. Further, [methyl- $^{13}\text{C}$ ]methionine NMR analysis of the R283A mutant form of Pol  $\beta$  would be expected to yield results with a Watson–Crick nascent base pair that are similar to the results reported here with DFT as the templating base. This mutant is known to be defective in catalysis, and the ternary complex crystal structure is in the open conformation (30). Dzantiev et al. (34) have previously studied the relationship between altered base pairing and enzyme conformation determined from limited proteolysis. Using this approach, they found that DFT in the templating position significantly reduced the stability of the closed *E. coli* Klenow fragment (exo<sup>−</sup>) ternary complex. In

contrast to Pol  $\beta$ , however, Klenow fragment, an A-family DNA polymerase, efficiently inserts dATP opposite DFT (27).

In summary, NMR studies of [methyl- $^{13}\text{C}$ ]methionine Pol  $\beta$  indicate that replacement of a templating thymine base with DFT, a thymine isostere, fails to support the large conformational change that is monitored by Met282. Interestingly, preliminary studies with a mispaired nucleotide yield qualitatively similar results, indicating a similar failure to activate the required conformational transition. The resonances of Met191 and Met155, located in the catalytic C-subdomain of the enzyme, show perturbations upon formation of the abortive ternary complex, which are qualitatively similar, but significantly weaker, than the changes observed when thymine is present at the templating base position. The changes in the Met155 and Met191 methyl resonances are in fact more similar to those observed in the binary Pol  $\beta$ –dATP complex. These studies demonstrate that the block in catalysis is directly related to the absence of the set of conformational transitions that include the “open” to “closed” transition monitored by Met282.

## ACKNOWLEDGMENT

We are grateful to Dr. Kasia Bebenek for many useful discussions on this project.

## SUPPORTING INFORMATION AVAILABLE

The Met236 resonance typically exhibited both shifted and unshifted resonances. The effect of increasing the nominal DNA:Pol  $\beta$  ratio on the Met236 methyl resonance is shown. This material is available free of charge via the Internet at <http://pubs.acs.org>.

## REFERENCES

1. Beard, W. A., and Wilson, S. H. (2000) Structural design of a eukaryotic DNA repair polymerase: DNA polymerase  $\beta$ , *Mutat. Res.* 460, 231–244.
2. Sawaya, M. R., Prasad, R., Wilson, S. H., Kraut, J., Pelletier, H. (1997) Crystal structures of human DNA polymerase  $\beta$  complexed with gapped and nicked DNA: Evidence for an induced fit mechanism, *Biochemistry* 36, 11205–11215.
3. Vande Berg, B. J., Beard, W. A., and Wilson, S. H. (2001) DNA structure and aspartate 276 influence nucleotide binding to human DNA polymerase  $\beta$ : Implication for the identity of the rate-limiting conformational change, *J. Biol. Chem.* 276, 3408–3416.
4. Yang, L., Beard, W. A., Wilson, S. H., Broyde, S., and Schlick, T. (2002) Polymerase  $\beta$  simulations suggest that Arg258 rotation is a slow step rather than large subdomain motions per se, *J. Mol. Biol.* 317, 679–699.
5. Yang, L., Beard, W. A., Wilson, S. H., Broyde, S., and Schlick, T. (2004) Highly organized but pliant active site of DNA polymerase  $\beta$ : Compensatory mechanisms in mutant enzymes revealed by dynamics simulations and energy analyses, *Biophys. J.* 86, 3392–3408.
6. Kim, S.-J., Beard, W. A., Harvey, J., Shock, D. D., Knutson, J. R., and Wilson, S. H. (2003) Rapid segmental and subdomain motions of DNA polymerase  $\beta$ , *J. Biol. Chem.* 278, 5072–5081.
7. Beard, W. A., Shock, D. D., and Wilson, S. H. (2004) Influence of DNA structure on DNA polymerase  $\beta$  active site function: Extension of mutagenic DNA intermediates, *J. Biol. Chem.* 279, 31921–31929.
8. Bose-Basu, B., DeRose, E. F., Kirby, T. W., Mueller, G. A., Beard, W. A., Wilson, S. H., and London, R. E. (2004) Dynamic characterization of a DNA repair enzyme: NMR studies of [methyl- $^{13}\text{C}$ ] methionine-labeled DNA polymerase  $\beta$ , *Biochemistry* 43, 8911–8922.
9. Prasad, R., Beard, W. A., and Wilson, S. H. (1994) Studies of gapped DNA substrate binding by mammalian DNA polymerase

- $\beta$ : Dependence on 5'-phosphate group, *J. Biol. Chem.* 269, 18096–18101.
10. Kool, E. T. (2002) Active site tightness and substrate fit in DNA replication, *Annu. Rev. Biochem.* 71, 191–219.
  11. Morales, J. C., and Kool, E. T. (2000) Varied molecular interactions at the active sites of several DNA polymerases: Non-polar isosteres as probes, *J. Am. Chem. Soc.* 122, 1001–1007.
  12. Schweitzer, B. A., and Kool, E. T. (1994) Aromatic nonpolar nucleosides as hydrophobic isosteres of pyrimidine and purine nucleosides, *J. Org. Chem.* 59, 7238–7242.
  13. John, B. K., Plant, D., and Hurd, R. E. (1993) Improved proton-detected heteronuclear correlation using gradient-enhanced Z and ZZ filters, *J. Magn. Reson.* 101, 113–117.
  14. Delaglio, F., Grzesiek, S., Vuister, G. W., Zhu, G., Pfeifer, J., and Bax, A. (1995) NMRPipe: A multidimensional spectral processing system based on UNIX pipes, *J. Biomol. NMR* 6, 277–293.
  15. Johnson, B. A., and Blevins, R. A. (1994) NMRView: A computer program for the visualization and analysis of NMR data, *J. Biomol. NMR* 4, 603–614.
  16. Zhu, G., and Bax, A. (1992) Improved linear prediction of damped NMR signals using modified forward backward linear prediction, *J. Magn. Reson.* 100, 202–207.
  17. Neal, S., Nip, A. M., Zhang, H., and Wishart, D. S. (2003) Rapid and accurate calculation of protein  $^1\text{H}$ ,  $^{13}\text{C}$ , and  $^{15}\text{N}$  chemical shifts, *J. Biomol. NMR* 26, 215–240.
  18. Xu, X. P., and Case, D. A. (2001) Automated prediction of N-15, C-13( $\alpha$ ), C-13( $\beta$ ) and C-13' chemical shifts in proteins using a density functional database, *J. Biomol. NMR* 21, 321–333.
  19. Xu, X. P., and Case, D. A. (2002) Probing multiple effects on N-15, C-13 $\alpha$ , C-13 $\beta$ , and C-13' chemical shifts in peptides using density functional theory, *Biopolymers* 65, 408–423.
  20. Hirao, I., Nishimura, Y., Naraoka, T., Watanabe, K., Arata, Y., and Miura, K. (1989) Extraordinary stable structure of short single-stranded-DNA fragments containing a specific base sequence—d(GCGAAGC), *Nucleic Acids Res.* 17, 2223–2231.
  21. Williams, H. E. L., Colgrave, M. L., and Searle, M. S. (2002) Drug recognition of a single DNA strand break; nogalamycin intercalation between coaxially stacked hairpins, *Eur. J. Biochem.* 269, 1726–1733.
  22. Beard, W. A., and Wilson, S. H. (2003) Structural insights into the origins of DNA polymerase fidelity, *Structure* 11, 489–496.
  23. Krahn, J. M., Beard, W. A., Miller, H., Grollman, A. P., and Wilson, S. H. (2003) Structure of DNA polymerase  $\beta$  with the mutagenic DNA lesion 8-oxodeoxyguanine reveals structural insights into its coding potential, *Structure* 11, 121–127.
  24. Krahn, J. M., Beard, W. A., and Wilson, S. H. (2004) Structural insights into DNA polymerase deterrents for misincorporation support an induced-fit mechanism for fidelity, *Structure* 12, 1823–1832.
  25. Beard, W. A., and Wilson, S. H. (2001) DNA lesion bypass polymerases open up, *Structure* 9, 759–764.
  26. Garcia-Diaz, M., Bebenek, K., Krahn, J. M., Blanco, L., Kunkel, T. A., and Pedersen, L. C. (2004) A structural solution for the DNA polymerase  $\lambda$ -dependent repair of DNA gaps with minimal homology, *Mol. Cell* 13, 561–572.
  27. Moran, S., Ren, R. X.-F., and Kool, E. T. (1997) A thymidine triphosphate shape analog lacking Watson–Crick pairing ability is replicated with high sequence selectivity, *Proc. Natl. Acad. Sci. U.S.A.* 94, 10506–10511.
  28. Moran, S., Ren, R. X.-F., Rumney, S., IV, and Kool, E. T. (1997) Difluorotoluene, a nonpolar isostere for thymine, codes specifically and efficiently for adenine in DNA replication, *J. Am. Chem. Soc.* 119, 2056–2057.
  29. Yang, L., Arora, K., Beard, W. A., Wilson, S. H., and Schlick, T. (2004) Critical role of magnesium ions in DNA polymerase  $\beta$ 's closing and active site assembly, *J. Am. Chem. Soc.* 126, 8441–8453.
  30. Beard, W. A., Osheroff, W. P., Prasad, R., Sawaya, M. R., Jaju, M., Wood, T. G., Kraut, J., Kunkel, T. A., and Wilson, S. H. (1996) Enzyme-DNA interactions required for efficient nucleotide incorporation and discrimination in human DNA polymerase  $\beta$ , *J. Biol. Chem.* 271, 12141–12144.
  31. Beard, W. A., Shock, D. D., Vande Berg, B. J., and Wilson, S. H. (2002) Efficiency of correct nucleotide insertion governs DNA polymerase fidelity, *J. Biol. Chem.* 277, 47393–47398.
  32. Osheroff, W. P., Beard, W. A., Wilson, S. H., and Kunkel, T. A. (1999) Base substitution specificity of DNA polymerase  $\beta$  depends on interactions in the DNA minor groove, *J. Biol. Chem.* 274, 20749–20752.
  33. Osheroff, W. P., Beard, W. A., Yin, S., Wilson, S. H., and Kunkel, T. A. (2000) Minor groove interactions at the DNA polymerase  $\beta$  active site modulate single-base deletion error rates, *J. Biol. Chem.* 275, 28033–28038.
  34. Dzantiev, L., Alekseyev, Y. O., Morales, J. C., Kool, E. T., and Romano, L. J. (2001) Significance of nucleobase shape complementarity and hydrogen bonding in the formation and stability of the closed polymerase-DNA complex, *Biochemistry* 40, 3215–3221.
  35. Beard, W. A., Shock, D. D., Yang, X.-P., DeLauder, S. F., and Wilson, S. H. (2002) Loss of DNA polymerase  $\beta$  stacking interactions with templating purines, but not pyrimidines, alters catalytic efficiency and fidelity, *J. Biol. Chem.* 277, 8235–8242.

BI0511742